JOURNAL OF APPLIED ELECTROCHEMISTRY 21 (1991) 877–884

Electrochemical investigations of the autophoretic coating process*

B. PFEIFFER, J. W. SCHULTZE

AGEF eV Arbeitsgemeinschaft Elektrochemischer Forschungsinstitutionen, Institut für Physikalische Chemie und Elektrochemie, Heinrich-Heine-Universität Düsseldorf, D-4000 Düsseldorf, FRG

Received 31 January 1991; revised 1 March 1991

Autophoretic coating (AC) is a complex chemical process consisting of various electrochemical partial reactions such as metal corrosion, hydrogen evolution and peroxide and oxygen reduction. While the redox potential of the bath is very positive, about 0.6 V, the coating process takes place at about −0.2 V dependent on the bath composition. The low conductivity of the bath is necessary to maintain the dispersion, but it hinders the kinetic investigations. Nevertheless potentiodynamic polarization curves show that the diffusion limited peroxide reduction and the corrosion of iron are the most important reactions. From the corrosion current density a maximum weight loss of 0.1 mg cm^{-2} is estimated for a standard film of 20 μm thickness. Hydrogen evolution is almost negligible during the first period of dipping. This conclusion can be justified by measurements in the hydrogen permeation cell. The partial current densities are not influenced by various emulgators, but the dispersion catalyses the hydrogen evolution and inhibits the anodic corrosion. The diffusion of peroxide is hindered. Potentiostatic measurements in various solutions show the role of ferrous ions deriving from corrosion in the case of iron or by reduction of ferric ions in the case of gold. Measurements at a disc electrode show that the cathodic reactions are dominated by diffusion and migration.

1. Introduction

The corrosion protection of steel made great progress due to the development of polymer electrode position processes. Important contributions were made by Beck [1, 2]. Autophoretic coating (AC) is a similar new industrial technology which simultaneously pretreats and coats metal surfaces [3, 4]. The metal is dipped into the coating bath for some minutes, washed in demineralized water and dried at 100° C. Like modern cathodic electrophoretic coating (EC) or cathodic electrodeposition of paint a colloidal dispersion is deposited at a metal surface by an electrochemical reaction. There are many similarities between these two technologies. In both systems the coating thickness is a function of time, and the process is applied to the metal surface. The thickness of the deposition generated is highly uniform. After drying, a very stable film with high corrosion protection properties is obtained. But in contrast to EC the external current is zero. While EC requires expensive electric equipment, AC exclusively uses chemical action to deposit the film-forming ingredients on the metal substrate.

For AC the coating bath consists of a water-borne "polymer dispersion" and a "starter". The coagulation process is started by pickling of the metal surface in a complexing acid containing an oxidizer. No organic solvent is needed. Polymers of high molecular weight can be used. The temperatures for film drying are low. The energy costs for depositing and cross-linking of the polymer can be saved. Any risk for workers, such as handling of high electric voltages, are avoided. Thus, in comparison to EC, many advantages arise, which favour future application of this technology [5, 6].

In spite of the very simple technology, the kinetics of the deposition reaction are rather complex. Few papers investigate the formal kinetic aspects e.g. the increase of rate with the concentration of peroxide or the film growth according to a square root law $d_{pol} \sim t^{1/2}$ [4–8] or the influence of the underlying metal. In this paper, we analyse the electrochemical kinetics of the corrosion reaction for iron as the most important metal compared with gold as an inert metal. The coagulation of the dispersion will be discussed in a paper to follow. A further important parameter is given by the nature of the polymer. Herein we only refer to polyvinylidenchloride which forms a stable film with optimum insulation properties.

2. Principles and analysis of the corrosion reaction

The "starter" contains a complexing acid (HF) and an oxidizer (H_2O_2). The corrosion process is expressed as follows [8, 9]:

$$Fe + z/2H_2O_2 + zH^+ \longrightarrow Fe^{z+} + zH_2O \quad (1)$$

where z = 2–3. The corrosion reactions under the

* This paper is dedicated to Professor Dr Fritz Beck on the occasion of this 60th birthday.

0021-891X/91 $03.00 + .12 © 1991 Chapman & Hall

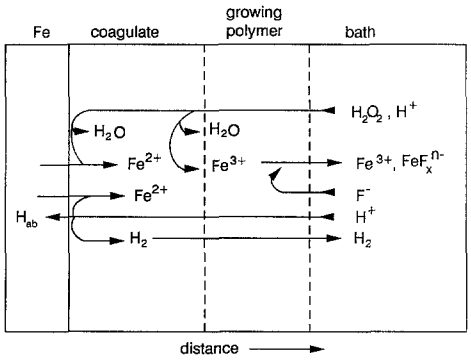

Fig. 1. Schematic representation of migration, diffusion and reactions in autophoretic coating.

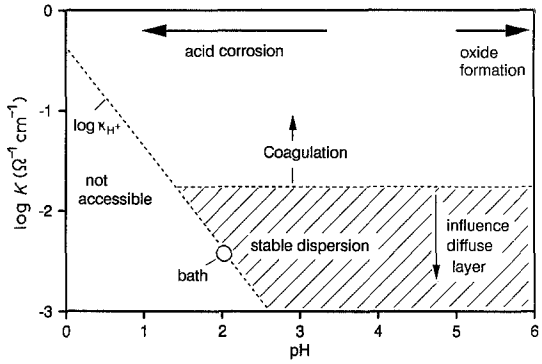

Fig. 3. Stability diagram of the polymer dispersion.

growing deposit are demonstrated in Fig. 1. The reaction is more complicated than described by Equation 1. For electrode reactions, which take place at a metal surface by charge transfer, the kinetics can be discussed in terms of the external current density, i, which is the sum of the partial current densities, expressed as

$$i(U) = \sum_{m=1}^{\infty} i_m^+(U) + \sum_{n=1}^{\infty} i_n^-(U) \qquad (2)$$

where i^+ and i^- are the anodic (corrosion) and cathodic (reduction) current densities of the partial reactions which depend on the potential U. For the special composition of the coating bath the partial reactions, given in Table 1, have to be considered. The equilibrium potentials of iron, hydrogen or the redox system, however, and the exchange current densities, i_0, are of minor importance. The technical process takes place at the corrosion potential, U_{corr}, where the external current density, i, is zero. This means that the anodic reaction of metal dissolution has to be compensated completely by the cathodic reactions of reduction of the oxidizer or hydrogen evolution.

Changing the electrode potential, U, the cathodic or anodic reactions are accelerated and can be analysed separately. This is shown in the speculative Fig. 2. The sign and the value of i give information on the rate of partial reactions taking place at the metal surface at a given U. By extrapolation of the current densities to U_{corr} the corrosion current density i_{corr} can be estimated. In pure HF-solution, U'_{corr} is determined by the Tafel lines of hydrogen evolution and anodic corrosion.

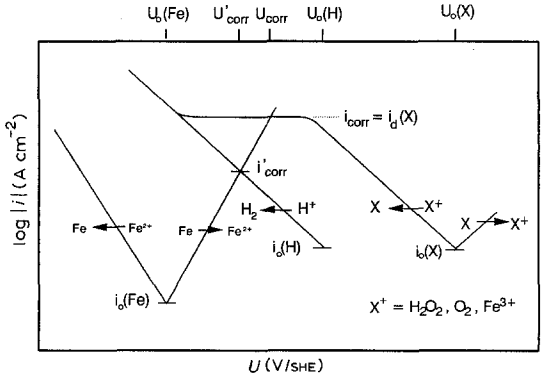

Fig. 2. Schematic diagram of partial current densities in the autophoretic coating process.

This process has two disadvantages: it is too slow, and the evolving hydrogen bubbles hinder the film formation. Hence, accelerators X^+ are added, which shift U to the more positive value $U_{corr} > U'_{corr}$ probably working in the region of diffusion limitation $i_d(X) = i_{corr}$. There are, however, no previous literature about these partial reactions.

The integral of i_{corr} over the dipping time t_{bath} is proportional to the quantity of the metal dissolved during the coating process.

$$m_{Fe} = \frac{M_{Fe}}{zF} \int_{t=0}^{t_{bath}} i_{corr}(t)\mathrm{d}t = \frac{M_{Fe} i_{corr} t_{bath}}{zF} \qquad (3)$$

2.1. *Electrochemistry in dilute solutions*

The aim of this paper is the investigation of the fundamental aspects of electrochemical kinetics. Such investigations should be carried out in an excess supporting electrolyte to exclude the effects of the diffuse double layer and to minimize the ohmic drop. In the case of AC, however, the necessary stability of the emulsion excludes salt concentrations exceeding 0.1 M. Figure 3 shows the influence of salt concentrations and pH. Acid solutions are necessary to achieve fast corrosion and coagulation. In neutral solutions, hydroxide formation takes place. The technical bath is located at the left edge of the stability region of the dispersion. (The region at the lower left edge is physically not accessible.)

Finally, the maintenance of a diffusion potential is important for the rate of the process. Therefore, the investigations were carried out in dilute solutions which may limit a straightforward kinetic analysis. Hence, approximations must be accepted for the analysis of the technical process.

3. Experimental details

3.1. *Autophoretic coating chemicals*

The concentrated polyvinylidenchloride latex (40% polymer solids by weight) was diluted to 0.5 to 10% latex. The latex was stabilised by anions such as sodiumlaurylsulphate ($[C_{12}H_{25}\text{–}OSO_3]Na$).

Two different starter systems were used. The first was a commercial AC-starter, applied by Henkel

KGaA Düsseldorf. The concentrated solution was diluted to 5% (by volume), in the following called "starter". To simulate the technical starter a second one was prepared by adding 0.1 M HF, 0.1 M H_2O_2 and 0.03 M $FeCl_3$. For special measurements the composition of this simulated starter could be varied. The influence of oxygen from the air on the corrosion process was analysed by bubbling nitrogen gas (99.999% N_2) through the solution and by using aerated solutions, respectively.

With both starter systems a standard coating bath was prepared, containing 5% polymer solids ("standard"). The deposited polymer layers of both baths were highly uniform and of good quality. For testing the bath, iron (Vacufer S1) and steel (ST 1405) panels were immersed in the stirred solution (magnetic stirrer 4 Hz) for 120 s. After removal from the bath the coating process was completed in air for 60–90 s, then the panels were washed in millipore water for 30 s. Afterwards they were dried with forced air circulation at 100° C for 1800 s. The thickness d_{pol} of the dried polymer was measured using a Minitest 2000 (measuring sonde F 400, Elektro-Physik, Köln). For standard conditions, d_{pol} was in the range of 20 $\pm$ 1 μm. Local deviations of thickness were less than 5%.

3.2. *Electrochemical measurements*

The electrode potential, U, was measured against a mercury/mercury sulphate electrode (0.680 V) in acid solution or a mercury/mercury oxide electrode (0.165 V) in alkaline solution. The reference electrodes were separated from the solution by a glass frit (G 4). All potentials given in this paper are referred to the standard hydrogen electrode (SHE).

Tafel plots were measured for the different electrode reactions with potentiodynamic sweep rates of 1 mV s^{-1} (Schiller potentiostat and IBM-AT microcomputer). To evaluate the contribution of a partial reaction to the overall process of corrosion, the composition of the starter solution was changed. Six different starter solutions were used: (a) 0.1 M HF (N_2); (b) 0.1 M HF, 0.1 M H_2O_2 (N_2); (c) 0.1 M HF, 0.03 M $FeCl_3$ (N_2); (d) 0.1 M HF, 0.2 atm O_2; (e) 0.1 M HF, 0.1 M H_2O_2, 0.03 M Fe^{3+}, 0.2 atm O_2 and (f) 5% standard starter, 0.2 atm O_2 ("starter").

Measurements under addition of the polymer dispersion gave the inhibitive effect of latex particles ("standard") or adsorbed emulgator molecules. In these solutions, however, film formation overlapped, the rate of the process decreasing with time. Therefore, the results refer to an intermediate time of about 30 s, in the case of potentiodynamic anodic measurements to $t \approx 50$ to 100 s.

For measurements at the rotating disc electrode iron and gold discs were fixed to a metal cylinder which was surrounded by a Teflon cover and the disc electrodes were fixed by Epoxid (Biphenol-A-Epichlorhydrin, Fa. Ciba Geigy). After drying the electrodes were polished. The standard rotation frequency, f, was 40 Hz.

Table 1. Partial reactions of the overall process of corrosion during autophoretic coating. (The equilibrium potentials are calculated for the actual composition of the coating bath)

	Fe-dissolution ($c_{Fe^{2+}} = 10^{-6}$ M) $Fe \rightarrow Fe^{2+} + 2e^-$	U_0 −0.62 V
	H_2-evolution (pH 2.3, $p_{H_2} = 1$ atm) (a) $H^+ + e^- \longrightarrow H_{ad} \longrightarrow \frac{1}{2}H_2$ ↓(b) H_{abs}	−0.14 V
	H_2O_2-reactions (pH 2.3, $c_{H_2O_2} = 0.1$ M $\frac{1}{2}H_2O_2 + H^+ + e^- \longrightarrow H_2O$	1.61 V
	O_2-reduction (pH 2.3, $p_{O_2} = 0.2$ atm)	
(a)	$O_2 + 4H^+ + 4e^- \longrightarrow 2H_2O$	1.09 V
(b)	$O_2 + 2H^+ + 2e^- \longrightarrow H_2O_2$	0.56 V
	Fe^{3+}-reduction ($c_{Fe^{3+}} = 0.03$ M, $c_{Fe^{2+}} = 10^{-6}$ M)	
(a)	pH < 2.43 $Fe^{3+} + e^- \longrightarrow Fe^{2+}$	1.04 V
(b)	pH > 2.43 $FeOH^{2+} + H^+ + e^- \longrightarrow Fe^{2+} + H_2O$	

3.3. *Permeation technique*

At iron or steel surfaces, cathodically produced hydrogen enters the metal (hydrogen embrittlement) causing a loss of rigidity. With permeation measurements a quantitative evaluation is possible [10, 11]. Therefore, the contribution of the hydrogen evolution to the process of corrosion can be estimated.

Two identical electrochemical cells were separated by a thin metal membrane ($d_{Fe} = 0.5$ mm). Hydrogen, produced at the cathodic side of the membrane, enters the metal (Table 1-2b) and diffuses to the rear side. At the anodic side the current density, i_{an}, was measured potentiostatically ($U_A = 0.22$ V, 0.1 M NaOH (N_2)). All hydrogen atoms are oxidized to protons, and the hydrogen concentration at this side is always zero. In order to protect the anodic side against corrosion, it was coated with a thin layer of palladium ($d_{Pd} = 0.1$ μm).

At the cathodic side hydrogen was produced potentiostatically at a negative potential ($U < U_{corr}$) or by free corrosion. If oxidizing agents are present, the adsorbed hydrogen atoms react (e.g., with oxygen) according to Equation 4 [11]:

$$2H_{ad} + \tfrac{1}{2}O_2 \longrightarrow H_2O \qquad (4)$$

and the cathodic hydrogen concentration is diminished. This can be seen by the decrease in the anodic current density, i_{an}.

4. Results

4.1. *Equilibrium and corrosion potential*

Open circuit potentials were measured in various solutions with the steel electrodes or inert gold elec-

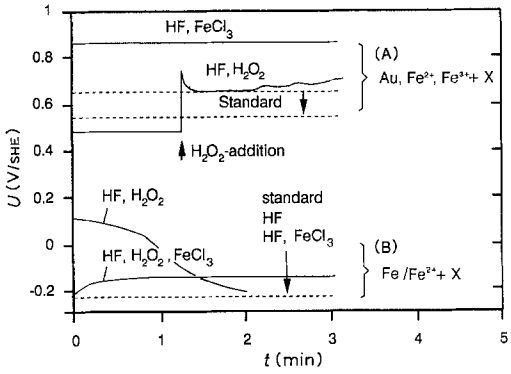

Fig. 4. (A) Equilibrium and (B) corrosion potential measured during autophoretic coating of Fe-electrodes. A polyvinyliden-chloride dispersion with 5% polymer solids was used with different concentration (a) of the "starter" (Henkel); (b) 0.1 M HF; (c) 0.1 M HF, 0.1 M H_2O_2; (d) 0.1 M HF, 0.03 M $FeCl_3$; (e) 0.1 M HF, 0.1 M H_2O_2, 0.03 $FeCl_3$.

trodes. Figure 4 shows typical time dependencies of potentials while Table 2 summarizes the average values. The potential of the gold electrode is about 0.8 to 1.0 V more positive than that of the steel electrode. This is due to the two different electrode reactions.

4.1.1. $Me/Fe^{2+}, Fe^{3+}$. For inert metals (Me = Au, Pt), the equilibrium potential is given by the redox couple. In the autophoretic coating process the potential is determined by Fe^{2+}/Fe^{3+} and H_2O_2.

$$2Fe^{2+} + 2H^+ + H_2O_2 = 2H_2O + 2Fe^{3+} \quad (5)$$

This potential can be calculated by applying the Nernst equation to the equilibrium reaction of Equation 5 taking into account the complexation of Fe^{3+} by F^-. In the technical process, the potential is measured for the control of the bath composition, it should be in the region of 0.6 V. The data of Table 2 show that the potential is shifted in the anodic direction by addition of oxygen, H_2O_2 and $FeCl_3$ or both. It is more positive than that of the technical bath which is due to complexation by F^--ions, or that of 0.1 M HF which has no oxidizing component.

4.1.2. Fe/Fe^{2+}. The corrosion potential (U_{corr} = −0.2 V) of the iron electrode can be roughly estimated by extrapolation of the cathodic and anodic Tafel lines in Fig. 2. Dependent on the cathodic reaction, the potential can be shifted by variation of the starter composition to U_{corr}. As Fig. 4 and Table 2 show, U_{corr} = −0.2 V is most negative in HF, but with addition of H_2O_2 and $FeCl_3$ it shifts in the anodic direction.

Table 2. Measurement of corrosion (Fe) and equilibrium (Au) potentials during autophoretic coating. (The values in brackets are for the pure starter without dispersion)

Different starter	*U* (V/SHE)	
	Fe/5% dispersion	*Au/5% dispersion*
"standard" bath (Henkel)	−0.22 (−0.26)	0.65/0.53*
0.1 M HF	−0.22 (−0.29)	0.49
0.1 M HF, O_2	−0.22	0.65
0.1 M HF, 0.1 M H_2O_2	+0.13/−0.22*	0.65
0.1 M HF, 0.03 M $FeCl_3$	−0.22	0.82
0.1 M HF, 0.1 M H_2O_2 0.03 M $FeCl_3$	−0.22/−0.16†	0.85

* potential shift by use of the bath in long terms
† potential shift at dipping time of 120 s

The corrosion potential of the metal in the pickling solution gives thermodynamic information as to which cathodic reactions can take place at the corroding metal surface (for equilibrium potentials calculated for the actual concentrations of the bath see Table 1). It follows, that all cathodic reactions of Table 1 can take place at the corroding iron surface.

4.2. *Contribution of partial reactions on the overall process of corrosion*

To evaluate the contribution of partial anodic and cathodic reactions, potentiodynamic measurements were carried out in 0.1 and 1 M HF, in the "starter" and in the "standard" bath. Current potential curves were recorded beginning at the corrosion potential. They are shown in Fig. 5 as Tafel plots. Quantitative data derived from Figs 5–8 are summarized in Table 3. Due to the low conductivity of the solutions, ohmic drops are high, and straight Tafel lines can be obtained up to several mA cm^{-2} only. Further, it should be pointed out that the diffusion conditions are ill-defined in the simulated technical process, since the forming polymer film disturbs the flow conditions at the disc electrode. Finally, in the film-forming solutions the concentration of adsorbates at the interface Fe/H_2O is not constant. Hence, quantitative results given in Table 3 should not be overemphasized.

In pure HF, at cathodic overpotentials, only hydrogen evolution is possible. Reasonable Tafel lines with transfer coefficients of 0.3 to 0.4 are obtained at current densities below 10 mA cm^{-2}. At high current densities the curves indicate the increasing ohmic drop.

The anodic Tafel lines correspond to the dissolution to Fe^{2+}-ions. At the surface the formation of Fe^{3+} is thermodynamically impossible. Oxidation according

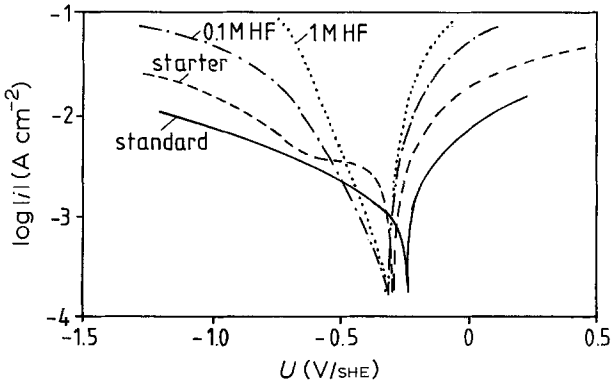

Fig. 5. Tafel lines obtained from i/U-measurements (sweep rate 1 mV s^{-1}, started at corrosion potential) at Fe-wires (diam. 0.5 mm, electropolished). Anodic reaction: Fe-dissolution. Cathodic reaction: H_2 evolution and H_2O_2-reduction. Stirred solutions (magnetic stirrer 4 Hz): 1 M HF (N_2) and 0.1 M HF (N_2); 5% "starter" (N_2) and autophoretic "standard" bath (N_2).

Table 3. Kinetic data of the partial reactions in the autophoretic coating bath (magnetic stirrer 4 Hz) obtained from potentiodynamic i/U-measurements shown in Fig. 5

System	U_{corr} (V)	i_{corr} ($mA\,cm^{-2}$)	$i_{diff}^{H_2O_2}$ ($mA\,cm^{-2}$)	b^- (mV)	α^-	b^+ (mV)	α^+
5% "starter"	−0.26	2.33	3.04	590	0.10	94	0.32 ($z = 2$) 0.21 ($z = 3$)
"standard" bath	−0.21	1.00	1.00	812	0.07	205	0.15
0.5 M H_2SO_4	−0.24	1.00	–	140	0.43	60	0.50
1 M HCl	−0.20	1.00	–	96	0.63	75	0.40
0.1 M HF	−0.30	0.25	–	195	0.30	60	0.50
1 M HF	−0.30	0.34	–	158	0.37	51	0.59
0.1 M HF 5% Polymer	−0.20	0.25	–	195	0.30	60	0.50
1 M HF 5% Polymer	−0.24	0.15	–	158	0.37	29	1.03

to Equation 5 takes place in the diffusion layer or in bulk solution only. At high anodic overpotentials ($U - U_{corr} > RT/zF = 25\,mV/z$) all cathodic reactions are negligible and the iron dissolution can be analysed separately. Tafel lines were obtained with a slope of $b^+ = 50$ to 60 mV (Fig. 5). With $z = 2$ in Equation 1 these slopes correspond to transfer coefficients, α^+, about 0.5, which are reasonable values for iron.

The corrosion current density obtained from Fig. 5 for HF is much less than in other acids (see Table 3). In the "starter" the hydrogen reaction is slower, but near the corrosion potential a cathodic step is observed which is due to the diffusion limited H_2O_2-reduction. The anodic reaction is slightly hindered. Hence the whole current/potential curve shifts in the anodic direction, but the extrapolated corrosion current density $i_{corr} = 2.3\,mA\,cm^{-2}$ is very high.

In the standard bath, the measurements are extremely difficult since the electrode is rapidly covered by the growing film. It can be easily seen, however, that the anodic reaction is slightly inhibited, as is also the cathodic H_2O_2 reaction. The corrosion potential shifts in the anodic direction, and i_{corr} remains in the milliampère range.

As a first approximation the acceleration of the cathodic reactions and anodic reactions in the starter solution and the standard bath can be explained by the superimposed diffusion current density of H_2O_2-reduction. The contribution of the hydrogen evolution to the overall process of corrosion is small ($i_{H^+} = 0.2$–$0.3\,mA\,cm^{-2}$). In the presence of H_2O_2 the corrosion reaction runs with much higher corrosion current density (0.1 M HF: $i_{corr} = 0.25\,mA\,cm^{-2}$; starter: $i_{corr} = 2.33\,mA\,cm^{-2}$).

This is a very important point for the coating process. Large cathodic current densities are necessary to compensate the corrosion process, but the hydrogen evolution must be suppressed. At current densities exceeding $1\,mA\,cm^{-2}$ H_2-bubbles are formed at the metal/coagulate interface, which may interrupt the polymer film [12].

Using Equation 3, the weight loss of iron during the AC-process was calculated. For a given film thickness of 20 μm it is less than $0.1\,mg\,cm^{-2}$, i.e. the iron removal by pickling is less than 0.5 μm. This can be correlated with the film growth [6]. The stoichiometric contribution of Fe^{2+} to the film composition is small, or negligible, as is typical for a coagulation process.

4.3. *Inhibition by latex particles*

The polymer dispersion contains latex particles with diameters in the range 0.02–02 μm. The transport of ions in the bath can be limited by these particles. The influence of the polymer dispersion on reactions, running with limited diffusion current density, has been analysed by changing the polymer concentration. These measurements are shown in Fig. 6. The diffusion current density of $3\,mA\,cm^{-2}$ in the starter

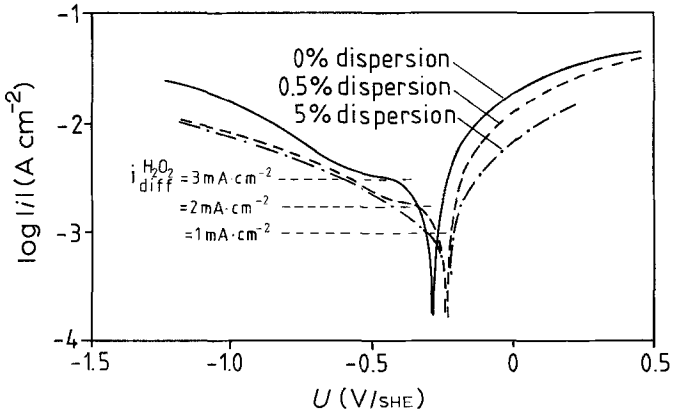

Fig. 6. Tafel plot for different concentrations of the polyvinylidenchloride dispersions. Standard "starter" solution containing 0%, 0.5% and 5% of polymer solids. Tafel lines are obtained from *i/U*-measurements (1 mV s^{-1}, magnetic stirrer 4 Hz, N_2-saturated) at Fe-wires (diam. 0.5 mm, electropolished). Diffusion current density of H_2O_2-reduction indicated.

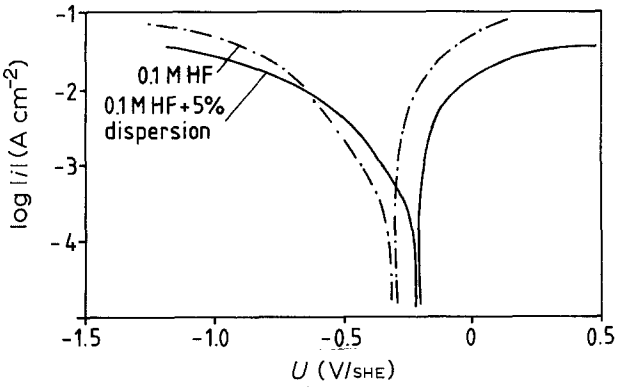

Fig. 7. Catalytic and inhibiting effect of the polyvinylidenchloride dispersion (1 mV s^{-1}, Fe-wires diam. 0.5 mm, electropolished). Stirred solutions (magnetic stirrer 4 Hz) containing (a) 0.1 M HF (N_2) and (b) 0.1 M HF (N_2) with 5% polymer solids.

solution is reduced to 1 mA cm^{-2} in the coating bath containing 5% polymer solids. Simultaneously, the anodic reaction is inhibited. As a consequence, U_{corr} shifts in the anodic direction.

In addition, the influence of the polymer dispersion on the hydrogen evolution has been analysed in the absence of H_2O_2 (Fig. 7). While this reaction is negligible in the starter solution, it increases with increasing polymer concentration. To suppress the hydrogen evolution the composition of the coating bath must be chosen carefully. The inhibition of the anodic reaction is again indicated by the anodic shift of U_{corr}.

4.4. *Test of inhibition by emulgator molecules*

The polymer dispersion is stabilised by emulgator molecules, adsorbed at the surface of the latex particles. By coagulation these emulgator molecules can be separated from the latex particle and adsorb at the metal surface. The inhibition or catalysis of the corrosion reaction by these surface active species is possible.

The influence of emulgator molecules has been measured at iron electrodes in 0.5 M sulphuric acid. Results are shown in Fig. 8. The anionic emulgators sodiumlaurylsulphate (LAU = [$C_{12}H_{25}$–OSO_3]Na), sulphosuccinate (SUL = R^1OOC–CH_2–$CH(SO_3Na)$–$COOR^2$), alkanesulphonate (ALK = [R–SO_2–O]Me) or phosphate emulgator (PHO) were tested in comparison to frequently used inhibitors like N-benzylchinoliniumchloride (BC = [C_9H_7N–CH_2–C_6H_5]Cl) and thiourea (TU = $SC(NH_2)_2$). To stabilize the dispersion 0.2 g dm^{-3} (10^{-3} M) of an emulgator is added. The inhibition effect, tested for all substances at this small concentration, was negligible. This is desired, because reasonable corrosion rates are necessary to get coagulate layers of good quality [4].

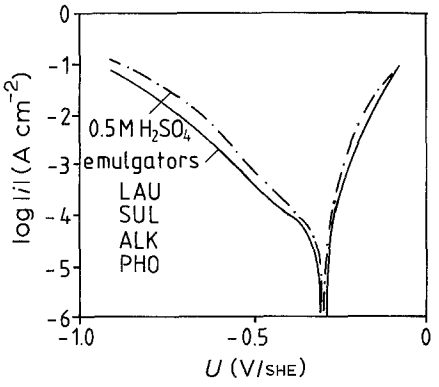

Fig. 8. Test of the inhibition effect of different emulgators (0.2 g dm^{-3}) on the active corrosion of iron in 0.5 M H_2SO_4. Emulgators: sodiumlaurylsulphate (LAU), alkansulphonate (ALK), sulphosuccinate (SUL), phosphate emulgator (PHO). Fe-wires (A = 0.5 cm^2), electropolished, stirring by N_2-bubbles.

4.5. *Potentiostatic layer formation*

To check the influence of the partial reactions on the real film growth, electrodes were potentiostatically painted for 30 s in various solutions with an optimum slow stirring rate of 4 Hz. Figures 9 and 10 show the results for gold and iron, respectively. The experiments with gold were useful, since the contribution of the corrosion could be eliminated. At gold no film growth was observed in the absence of $FeCl_3$, but thin films could be formed in its presence (reduction of Fe^{3+} to Fe^{2+}). This proves the role of Fe^{2+}-ions for the coagulation. The potential dependence is almost negligible since the deposition takes place under diffusion control.

In contrast, fast film formation takes place at iron, since Fe^{2+} ions are formed by anodic corrosion which can be compensated by the reduction of Fe^{3+} or H_2O_2. Here again the dominance of Fe^{2+}-ions for the coagulation process can be shown with the experiment in HF. On the cathodic side without corrosion, film growth is impossible. Anodic dissolution, however, causes the coagulation.

The correlation with the current potential curves at

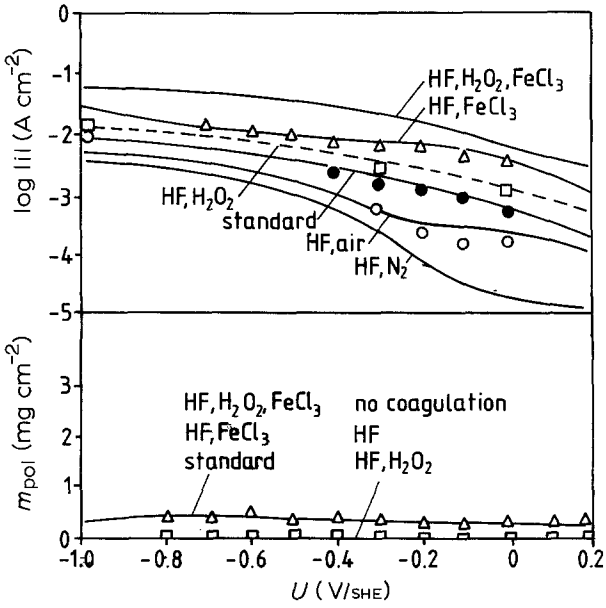

Fig. 9. Film weight at the Au-electrode after potentiostatic polarization for 30 s, magnetic stirrer 4 Hz. 5% dispersion with various starters: (a) 0.1 M HF; (b) 0.1 M HF, 0.1 M H_2O_2; (c) 0.1 M HF, 0.03 M $FeCl_3$; (d) 0.1 M HF, 0.1 M H_2O_2, 0.03 $FeCl_3$. Upper part: Tafel diagram for the starters without dispersion at the rotating gold disc electrode at 40 Hz.

the rotating disc electrode will be discussed in the next section.

4.6. *Diffusion current densities*

To analyse the cathodic diffusion current densities a rotating disc electrode was used. The solutions, however, were used without the latex only. Results of potentiodynamic measurements at 40 Hz are shown in the upper part of Fig. 9 for gold.

The oxygen reduction was measured in aerated 0.1 M HF (0.2 atm O_2), compared to nitrogen saturated HF. The step between 0 and -0.2 V shows the expected diffusion limited current. Increasing current densities are observed for a standard starter, H_2O_2, $FeCl_3$ or both. The diffusion limitation is not so pronounced as usual due to the dilute electrolyte with low conductivity. In the case of reduction of protons or ferric ions, the migration overlaps the diffusion.

For iron electrodes, the correspondent curves are shown in the upper part of Fig. 10. Here, however, in addition to the cathodic reactions, anodic iron dissolution is also seen.

4.7. *Permeation measurements*

It was concluded above that in the technical process cathodic hydrogen evolution is substituted by the reduction of the accelerator H_2O_2. To check this conclusion, measurements in the permeation cell were carried out.

Initially, the measuring cell (cathodic side) was empty, but the anodic side was used normally. After removal of all hydrogen from the metal membrane (10 h) a very small anodic current density $i_A = 50\,\mathrm{nA\,cm^{-2}}$ was measured. The investigated electrolyte was placed in the cathodic compartment of the double cell. Corrosion took place immediately, as observed by establishment of the corrosion potential.

To check the method 0.1 M HF was initially used

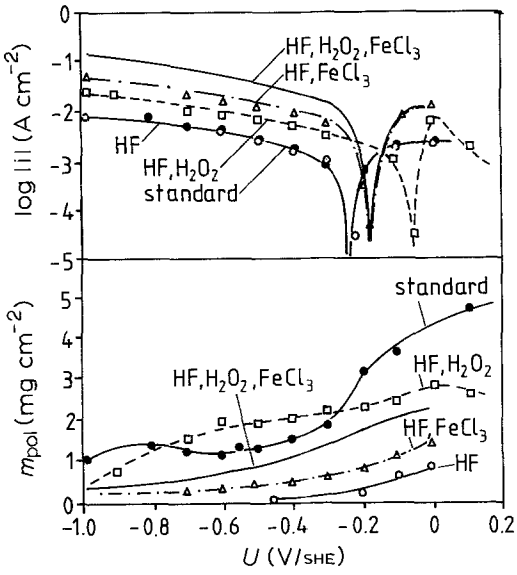

Fig. 10. Same measurement as in Fig. 9 at Fe-electrodes.

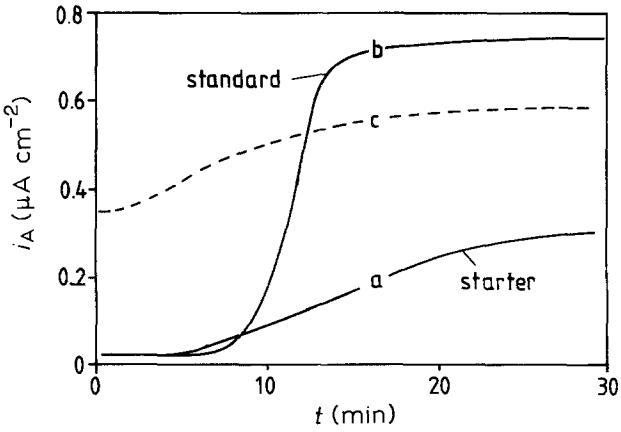

Fig. 11. Permeation curves measured during coating process. The permeation current density i_A, measured at the rear side of an iron membrane, is a function of hydrogen, adsorbed at the cathodic side of the membrane. (a) Standard "starter", (b) "standard" bath, (c) starter until i_A is constant (300 s), than addition of an corresponding amount of the dispersion (5% polymer solids in bath).

(not shown in Fig. 11). In this case the cathodic reaction was pure hydrogen evolution. The penetration time for hydrogen diffusion through the metal membrane was 190 s. After 300 s the stationary permeation current density $i_A^\infty = 3\,\mu\mathrm{A\,cm^{-2}}$ was established.

Thus, in the starter solution, during the immersion time of 120 s, no hydrogen penetration can be seen. Therefore the analysis of a time interval exceeding 5 min is necessary. After 300 s a small amount of hydrogen permeation took place. This observation can be explained by the oxidation of any H_{ad} by H_2O_2. Hydrogen evolution does not take place. This is an additional proof for our prediction that the autophoretic corrosion reaction takes place according to Equation 1 without hydrogen evolution.

The catalysis of the hydrogen evolution by the polymer dispersion, predicted from the results of Fig. 7 can also be seen in this experiment. If the polymer dispersion is added to the starter (Curve c in Fig. 9) or if the standard coating bath is used (Curve b), the stationary permeation current density i_A^∞ increases by a factor of three.

5. Discussion

The corrosion of iron in the autophoretic coating bath depends on the cathodic reaction. The kinetics of these reactions have been analysed. The rate of corrosion can be described according to Equation 6:

$$i_{corr}(U_{corr}) = i_{Fe}^{+}(U) = |i_{H^+}^{-}|(U) + |i_{Fe^{2+}}^{-}|(U) + |i_{diff}^{-}|(c) \quad (6)$$

$$i_{diff}^{-}(c) = i_{H_2O_2}^{-}(c) + i_{O_2}^{-}(c) + i_{Fe^{3+}}^{-}(c) \quad (7)$$

With potential/time measurements the thermodynamic possibility (depending on the equilibrium potential of redox couple and the corrosion potential of the metal) of these cathodic reactions, taking place at the corroding metal surface, has been checked. Potentiodynamic current potential measurement gave the rate of these reactions. The kinetic data are summarised in Table 3.

At corrosion potential the dominating cathodic reaction is H_2O_2-reduction. In addition, this has been proved in the permeation cell. The H_2O_2-reduction is limited by diffusion. The diffusion current densities of Fe^{3+}-reduction have to be taken into account, too, while that of oxygen is small due to its low concentration. The corrosion current density is limited by the sum of these three reactions. Hydrogen evolution can be neglected. Addition of the polymer dispersion decreases the diffusion current density and thereby the corrosion current density.

Destabilisation of the dispersion causes coagulation onto the metal surface. The stability of the dispersion is a function of ionic strength of the solution and pH, shown in Fig. 3. Due to corrosion, these parameters in the diffusion layer are very different than in bulk of solution. The importance of corrosion kinetics for the autophoretic coating process can be summarized under 5 headings:

(i) $i_{corr} = f(\Sigma i^-)$. For the coagulation process fast corrosion (high corrosion current density) is needed. The value of i_{corr} depends on the cathodic reactions. While the rate of reactions, limited mainly by diffusion, are reduced with increasing polymer concentration, the hydrogen evolution is catalysed. At high current densities bubbles are formed at the interface Fe/coagulate, which interrupt the polymer film. This should be avoided.

(ii) $m_{Latex} = f(i_{corr})$. Due to rapid corrosion a diffusion layer at the metal surface is established. The conductivity of the bath is low (2–3 mS cm^{-1}). From the very different concentration and transport properties of ions like Fe^{2+} and OH^-, produced by corrosion, a diffusion potential arises. Thus a field results which causes an acceleration of the transport of the highly charged latex particles to the metal surface by nearly one order of magnitude [13]. The accelerated deposition of latex particles depends on the corrosion process.

(iii) $m_{Fe} = f(i_{corr})$. The adherence and quality (colour, corrosion resistance) of the paint, retained after drying the coagulate layer, depends on the corrosion of the metal surface. For the coating bath a corrosion current density of 1 mA cm^{-2} has been measured. The very small quantity of metal dissolved during the coating process has been estimated to be $m_{Fe} < 0.1$ mg cm^{-2}.

(iv) $i_{corr} = constant \neq f(t_{bath})$. The homogeneity of deposit requires a self inhibiting mechanism. Parts of the metal surface, which have been coated quickly at the beginning of the coating process, grow slowly. The corrosion current density is constant during the coating process. This means that the inhibition effect cannot be explained by diffusion of ferrous ions through the coagulate deposit. On the other hand, with increasing thickness of coagulate (increasing distance to the metal surface, where ions are produced by corrosion) the field strength, generated by the diffusion potential, decreases. With growing coating thickness the acceleration of latex transport by migration is reduced.

(v) $z = 2$. Only Fe^{2+} is formed by corrosion. This causes the deposition of the latex near the surface. In the bulk solution, of course, ferrous ions must immediately be oxidized to guarantee the bath stability. Therefore the oxidation potential must be controlled during the process.

Acknowledgement

The support of this work by the Firma Henkel KGaA Düsseldorf is gratefully acknowledged. The authors wish to thank Dr D. Oberkobusch and Dr H. Fischer (Firma Henkel KGaA Düsseldorf) for fruitful discussions and preparation of autophoretic chemicals.

References

[1] F. Beck, *Progr. Org. Coatings* **4** (1976) 1.
[2] *Idem., Makromol. Chem., Macromol. Symp.* **8** (1987) 285.
[3] L. Steinbrecher and W. Hall, U.S. Patent 3 592 699 and U.S. Patent 3 585 084 (1971).
[4] J. Munz and L. Dulog, *Angew. Makromol. Chem.* **125** (1984) 87.
[5] B. Pfeiffer, Thesis, Unversity of Düsseldorf (1990).
[6] B. Pfeiffer and J. W. Schultze, *Bänder, Bleche Rohre* **10** (1990) 163.
[7] D. C. Prieve, R. S. Smith, R. A. Sander and H. L. Gerhart, *J. Coll. Interf. Sci.* **71** (1979) 267.
[8] D. C. Prieve, H. L. Gerhart and R. E. Smith, *Ind. Eng. Chem. Prod. Res. Dev.* **17** (1978) 32.
[9] J. W. Prane, *Polymer News* **4** (1977) 79.
[10] M. D. Archer and N. C. Grant, *Proc. Roy. Soc., Lond.* **A395** (1984) 165.
[11] E. Riecke and B. Johnen, *Werkstoffe und Korrosion* **37** (1986) 310.
[12] B. Pfeiffer, A. Thyssen and J. W. Schultze, *J. Electroanal. Chem.* **260** (1989) 393.
[13] R. E. Smith and D. C. Prieve, *Chem. Eng. Sci.* **37** (1982) 1213.